EUROPEAN ORGANIZATION FOR NUCLEAR RESEARCH

CERN-EP/2002-035
May 16, 2002

Measurement of Genuine Three-Particle Bose-Einstein Correlations in Hadronic Z Decay

L3 Collaboration

Abstract

We measure three-particle Bose-Einstein correlations in hadronic Z decay with the L3 detector at LEP. Genuine three-particle Bose-Einstein correlations are observed. By comparing two- and three-particle correlations we find that the data are consistent with fully incoherent pion production.

Submitted to *Phys. Lett. B*

Introduction

So far, no theory exists which can describe the non-perturbative process of hadron production in general and Bose-Einstein (BE) effects in particular. The latter are expected from general spin statistics considerations. To help understand these phenomena, studies of identical-boson correlations in e^+e^- collisions at LEP have been performed in terms of the absolute four-momentum difference Q [1], as well as in two- and three-dimensional distributions in components of Q [2,3].

It has long been realized that the shape and size in space-time of a source of pions can be determined, as a consequence of the interference of identical bosons, from the shape and size of the correlation function of two identical pions in energy-momentum space [4]. Additional information can be derived from higher-order correlations. Furthermore, such correlations constitute an important theoretical issue for the understanding of Bose-Einstein correlations (BEC) [5].

In this Letter three-particle correlations are analysed. These correlations are sensitive to asymmetries in the particle production mechanism [6,7] which cannot be studied by two-particle correlations. In addition, the combination of two- and three-particle correlation analyses gives access to the degree of coherence of pion production [8,9], which is very difficult to investigate from two-particle correlations alone due to the effect of long-lived resonances on the correlation function. The DELPHI [10] and OPAL [11] collaborations have both studied three-particle correlations but did not investigate the degree of coherence.

The Data and Monte Carlo

The data used in this analysis were collected by the L3 detector [12] in 1994 at a centre-of-mass energy of 91.2 GeV and correspond to a total integrated luminosity of 48.1 pb^{-1}. The Monte Carlo (MC) event generators JETSET [13] and HERWIG [14] are used to simulate the signal process. Within JETSET, BEC are simulated using the BE_0 algorithm [15,16] [1]. The generated events are passed through the L3 detector simulation program, which is based on the GEANT [17] and GHEISHA [18] programs, reconstructed and subjected to the same selection criteria as the data.

The event selection is identical to that presented in Reference 2, resulting in about one million hadronic Z decay events, with an average track multiplicity of about 12. Two additional cuts are performed in order to reduce the dependence of the detector correction on the MC model used: tracks with measured momentum greater than 1 GeV are rejected, as are pairs of like-sign tracks with opening angle below 3°. This results in an average track multiplicity of about 7. For the computation of three-particle correlations, each possible triplet of like-sign tracks is used to compute the variable $Q_3 \equiv \sqrt{Q_{12}^2 + Q_{23}^2 + Q_{31}^2}$, where $Q_{ij} \equiv \sqrt{-(p_i - p_j)^2}$ is the absolute four-momentum difference between particles i and j. Since Q_{ij}, and thus Q_3, depends both on the energy of the particles and on the angle between them, small Q_{ij} can be due to small angles or low energies. In a MC generator with BE effects, the fraction of pairs at small Q_{ij} with small angle is larger than in one without. Consequently, the estimated detection efficiency depends on the MC model used. The momentum and opening angle cuts reduce this model dependence. After selection, the average triplet multiplicity is about 6. In

[1] The Bose-Einstein simulation is done by the subroutine LUBOEI, with the values PARJ(92)=1.5 and PARJ(93)=0.33 GeV.

the region of interest, $Q_3 < 1$ GeV, the loss of triplets by the momentum and opening angle cut is about 40%.

The momentum cut improves the resolution of Q_3 by a factor three with respect to that for the full momentum spectrum. Using MC events, its average is estimated to be 26 MeV for triplets of tracks with $Q_3 < 0.8$ GeV. We choose a bin size of 40 MeV, somewhat larger than this resolution.

In Figure 1, the data are compared to JETSET (with and without BE effects) and HERWIG (not having a BE option) at the detector level, after performing all the cuts mentioned above, in the three-particle distributions $\sum \delta\phi$, $\sum \delta\theta$, and Q_3. The sums run over the three pairs of like-sign tracks in the triplet and $\delta\phi$ and $\delta\theta$ are the absolute differences in azimuthal and polar angle between two tracks, respectively. Within 10%, the angular distributions of the MC models agree with those of the data. None of the models describes the Q_3 distribution: JETSET with BE effects overestimates the data by approximately 20% at low Q_3, even though we found good agreement for $\delta\phi$, $\delta\theta$, and Q [2]. JETSET without BE effects and HERWIG grossly underestimate the data at low Q_3. The statistics for $Q_3 < 160$ MeV are so poor, that this region is rejected from the analysis.

The Analysis

The three-particle number density $\rho_3(p_1, p_2, p_3)$ of particles with four-momenta p_1, p_2 and p_3 can be described in terms of single-particle, two-particle and genuine three-particle densities as

$$\rho_3(p_1,p_2,p_3) = \rho_1(p_1)\rho_1(p_2)\rho_1(p_3) + \sum_{(3)} \{\rho_1(p_1)\left[\rho_2(p_2,p_3) - \rho_1(p_2)\rho_1(p_3)\right]\} + C_3(p_1,p_2,p_3) \quad , \quad (1)$$

where the sum is over the three possible permutations and C_3 is the third-order cumulant, which measures the genuine three-particle correlations. The $\rho_1\rho_2$ terms contain all the two-particle correlations. In order to focus on the correlation due to BE interference, we replace products of single-particle densities by the corresponding two- or three-particle density, ρ_0, which would occur in the absence of BEC, and define the correlation functions

$$R_2(p_1,p_2) \equiv \frac{\rho_2(p_1,p_2)}{\rho_0(p_1,p_2)} \quad , \qquad R_3(p_1,p_2,p_3) \equiv \frac{\rho_3(p_1,p_2,p_3)}{\rho_0(p_1,p_2,p_3)} \quad . \quad (2)$$

Assuming the absence of two-particle correlations, *i.e.*, $\rho_2(p_1,p_2) = \rho_1(p_1)\rho_1(p_2)$, results in

$$R_3^{\mathrm{genuine}}(p_1,p_2,p_3) \equiv 1 + \frac{C_3(p_1,p_2,p_3)}{\rho_0(p_1,p_2,p_3)} \quad . \quad (3)$$

The kinematical variable Q_3 is used to study three-particle correlations. For a three-pion system, $Q_3 = \sqrt{M_{123}^2 - 9m_\pi^2}$, with M_{123} the invariant mass of the pion triplet and m_π the mass of the pion. In this Letter, ρ_3 is defined as

$$\rho_3(Q_3) \equiv \frac{1}{N_{\mathrm{ev}}} \frac{\mathrm{d}n_{\mathrm{triplets}}}{\mathrm{d}Q_3} \quad , \quad (4)$$

with N_{ev} the number of selected events and n_{triplets} the number of triplets of like-sign tracks, and ρ_2 is defined analoguously.

Assuming totally incoherent production of particles and a source density $f(x)$ in space-time with no dependence on the four-momentum of the emitted particle, the BE correlation functions is related to the source density by [8, 19]

$$R_2(Q_{ij}) = 1 + |F(Q_{ij})|^2 \tag{5}$$

$$\begin{aligned} R_3(Q_{12}, Q_{23}, Q_{31}) &= 1 + |F(Q_{12})|^2 + |F(Q_{23})|^2 + |F(Q_{31})|^2 \\ &\quad + 2\,\mathrm{Re}\{F(Q_{12})F(Q_{23})F(Q_{31})\} \end{aligned} \tag{6}$$

$$R_3^{\mathrm{genuine}}(Q_{12}, Q_{23}, Q_{31}) = 1 + 2\,\mathrm{Re}\{F(Q_{12})F(Q_{23})F(Q_{31})\} \tag{7}$$

where $F(Q_{ij})$ is the Fourier transform of $f(x)$.

R_2 does not depend on the phase ϕ_{ij} contained in $F(Q_{ij}) \equiv |F(Q_{ij})| \exp(\iota\phi_{ij})$. However, this phase survives in the three-particle BE correlation functions, Equations (6) and (7). Assuming fully incoherent particle production, the phase ϕ_{ij} can be non-zero only if the space-time distribution of the source is asymmetric and $Q_{ij} > 0$. Defining

$$\omega(Q_{12}, Q_{23}, Q_{31}) = \frac{R_3^{\mathrm{genuine}}(Q_{12}, Q_{23}, Q_{31}) - 1}{2\sqrt{(R_2(Q_{12}) - 1)(R_2(Q_{23}) - 1)(R_2(Q_{31}) - 1)}} \quad , \tag{8}$$

then for an incoherent source Equations (5) and (7) imply that $\omega = \cos\phi$, where $\phi \equiv \phi_{12} + \phi_{23} + \phi_{31}$. Furthermore, as $Q_{ij} \to 0$, then $\phi_{ij} \to 0$, and hence $\omega \to 1$. For $Q_{ij} > 0$, a deviation from unity can be caused by an asymmetry in the production. However, this will only result in a small (a few percent) reduction of ω [6, 7], and this only in the case where the asymmetry occurs around the point of highest emissivity. It is important to emphasize that for (partially) coherent sources, ω can still be defined by Equation (8), but Equations (5–7) are no longer valid, in which case more complicated expressions are needed [7], and one can no longer deduce that $\omega = \cos\phi$ or that $\omega \to 1$ as $Q_{ij} \to 0$. In at least one type of model, one can make the stronger statement that the limit $\omega = 1$ at $Q_{ij} \to 0$ can only be reached if the source is fully incoherent [20].

Determination of R_3 and R_3^{genuine}

The reference sample, from which ρ_0 is determined, is formed by mixing particles from different data events in the following way. Firstly, 1000 events are rotated to a system with the z-axis along the thrust axis and are stored in a "pool". Then, tracks of each new event outside the pool are exchanged with tracks of the same charge from events in the pool having about the same (within about 20%) multiplicity, under the condition that all tracks originate from different events. Thus, after this procedure the new event consists of tracks originating from different events in the pool, and its original tracks have entered the pool. This updating process prevents any regularities in the reference sample. Finally, Q_3 is calculated for each triplet of like-sign tracks, resulting in the density ρ_{mix}.

This mixing procedure removes more correlations than just those of BE, *e.g.*, those from energy-momentum conservation and from resonances. This effect is estimated using a MC model with no BE effects (JETSET or HERWIG) at generator level and using pions only. Thus, in the absence of BEC, the corrected three-particle density is given by

$$\rho_0(Q_3) = \rho_{\mathrm{mix}}(Q_3)\mathcal{C}_{\mathrm{mix}}(Q_3), \quad \text{where } \mathcal{C}_{\mathrm{mix}}(Q_3) = \left[\frac{\rho_3(Q_3)}{\rho_{\mathrm{mix}}(Q_3)}\right]_{\mathrm{MC,noBE}} \quad . \tag{9}$$

The density ρ_3, measured in data, must be corrected for detector resolution, acceptance, efficiency and for particle misidentification. For this we use a multiplicative factor, $\mathcal{C}_{\text{det}}$, derived from MC studies. Since no hadrons are identified in the analysis, $\mathcal{C}_{\text{det}}$ is given by the ratio of the three-pion correlation function found from MC events at generator level to the three-particle correlation function found using all particles after full detector simulation, reconstruction and selection. Combining this correction factor with Equations (2) and (9) results in

$$R_3(Q_3) = \frac{\rho_3(Q_3)\,\mathcal{C}_{\text{det}}(Q_3)}{\rho_{\text{mix}}(Q_3)\,\mathcal{C}_{\text{mix}}(Q_3)} \quad . \tag{10}$$

The genuine three-particle BE correlation function, R_3^{genuine}, is obtained via

$$R_3^{\text{genuine}} = R_3 - R_{1,2} + 1 \quad , \tag{11}$$

where $R_{1,2} \equiv (\sum \rho_1\rho_2)/\rho_0 - 2$ is the contribution due to two-particle correlations, as may be seen from Equations (1) and (2). The product of densities $\sum \rho_1(p_1)\rho_2(p_2, p_3)$ is determined by a similar mixing procedure, as defined earlier, where two like-sign tracks from the same event are combined with one track having the same charge from another event with the same multiplicity. Finally, the variable Q_3 is calculated from these three tracks. This procedure is similar to that given in Reference 21. The ratio $(\sum \rho_1\rho_2)/\rho_0$ is also corrected for detector effects as ρ_3/ρ_{mix}.

In our analysis, we use JETSET without BEC and HERWIG to determine $\mathcal{C}_{\text{mix}}$ and JETSET with and without BEC as well as HERWIG to determine $\mathcal{C}_{\text{det}}$. These six MC combinations serve to estimate systematic uncertainties. The corrections are largest at small Q_3. At $Q_3 = 0.16$ GeV, these corrections to R_3 are $\mathcal{C}_{\text{mix}} \approx$ 5–30% and $\mathcal{C}_{\text{det}} \approx$ 20–30%, depending on which MC is used. These corrections for R_3 and $R_{1,2}$ are correlated and largely cancel in calculating R_3^{genuine} by Equation (11).

To correct the data for two-pion Coulomb repulsion in calculating ρ_2, each pair of pions is weighted by the inverse Gamow factor [22]

$$G_2^{-1}(\eta_{ij}) = \frac{\exp(2\pi\eta_{ij}) - 1}{2\pi\eta_{ij}}, \quad \text{where} \quad \eta_{ij} = \frac{m_\pi \alpha}{Q_{ij}} \tag{12}$$

and α is the fine-structure constant. It has been shown [23] that this Gamow factor is an approximation suitable for our purposes. For ρ_3, the weight of each triplet is taken as the product of the weights of the three pairs within it. For $\sum \rho_2\rho_1$ we use the same weight but with $G_2(Q_{ij}) \equiv 1$ when particles i and j come from different events. At the lowest Q_3 values under consideration, the Coulomb correction is approximately 10%, 3% and 2%, for ρ_3, $\sum \rho_1\rho_2$ and ρ_2, respectively.

Results

The measurements of R_3, $R_{1,2}$ and R_2 are shown in Figure 2. The full circles correspond to the averages of the data points obtained from the six possible MC combinations used to determine $\mathcal{C}_{\text{mix}}$ and $\mathcal{C}_{\text{det}}$. The error bars, σ_1, include both the statistical uncertainty and the systematic uncertainty of the MC modeling, which is taken as the r.m.s. of the values obtained using the different MC combinations. This dominant systematic uncertainty is, for $Q_3 < 0.8$ GeV, about a factor 5 to 7 larger than the statistical uncertainty and is correlated between the R_3, $R_{1,2}$ and R_2 distributions of Figure 2 and between bins. Figure 2a shows the existence of three-particle correlations and from Figure 2b it is clear that about half is due to two-particle correlations. Figure 2c shows the two-particle correlations.

As a check, R_3, $R_{1,2}$ and R_2 are also computed for MC models without BEC, both HERWIG and JETSET, after detector simulation, reconstruction and selection. For the mixing and detector corrections all possible MC combinations, giving non-trivial results, are studied. The results of this check are shown in Figure 2 as open circles and, as expected, flat distributions around unity are observed.

Figure 3a shows the genuine three-particle BE correlation function R_3^{genuine}. The data points show the existence of genuine three-particle BE correlations. The MC systematic uncertainty is highly correlated from bin to bin. At $Q_3 < 0.8$ GeV, it is about a factor 1.5 to 3.5 larger than the statistical uncertainty, the higher value corresponding to the lowest Q_3 value used. The open circles correspond to MC without BEC and form a flat distribution around unity, as expected.

Gaussian Parametrizations

A fit from $Q_3 = 0.16$ to $1.40\,\text{GeV}$ using the covariance matrix including both the statistical uncertainty and the systematic uncertainty due to the MC modeling, σ_1, is performed on the data points with the commonly used [8, 10, 11, 21] parametrization

$$R_3^{\text{genuine}}(Q_3) = \tilde{\gamma}\left[1 + 2\tilde{\lambda}^{1.5}\exp(-\tilde{R}^2 Q_3^2/2)\right](1 + \tilde{\varepsilon} Q_3) \quad , \tag{13}$$

where $\tilde{\gamma}$ is an overall normalization factor, $\tilde{\lambda}$ measures the strength of the correlation, $\tilde{R}$ is a measure for the effective source size in space-time and the term $(1 + \tilde{\varepsilon} Q_3)$ takes into account possible long-range momentum correlations. The form of this parametrization is a consequence of the assumptions that $\omega = 1$ and that $|F(Q_{ij})| = \sqrt{\lambda}\exp(-\tilde{R}^2 Q_{ij}^2/2)$, as would be expected for a Gaussian source density. The fit results are given in the first column of Table 1 and shown as the full line in Figure 3a.

In addition to the MC modeling, we investigate four other sources of systematic uncertainties on the fit parameters. Firstly, the influence of a different mixing sample is studied by removing the conditions that tracks are replaced by tracks with the same charge and coming from events with approximately the same multiplicity. For each of the six MC combinations, the difference in the fit results between the two mixing methods is taken as an estimate of the systematic uncertainty. The square root of the mean of the squares of these differences is assigned as the systematic uncertainty from this source. In the same way, systematic uncertainties related to track and event selection and to the choice of the fit range are evaluated. The analysis is repeated with stronger and weaker selection criteria, changing the number of events by about $\pm 11\%$ and the number of tracks by about $\pm 12\%$. The fit range is varied by removing the first point of the fit and varying the end point by ± 200 MeV. Finally, we study the influence of removing like-sign track pairs with small polar and azimuthal opening angles. The maximum deviation that is found by varying the cuts on these angles up to 6°, is taken as the systematic uncertainty from this source. The total systematic uncertainty due to these four sources is obtained by adding the four uncertainties in quadrature. We refer to this systematic uncertainty as σ_2. For all fit parameters, the largest part of the total uncertainty is due to the six possible combinations of mixing and detector MC corrections and amounts to 50 to 90%. Table 2 shows the uncertainties for each of the sources for the fit parameters of Equation (13).

As a cross-check, the analysis is repeated without the momentum cut of $1\,\text{GeV}$ and without the cut of 3° on the opening angle of like-sign track pairs. The results agree with those given in Table 1 well within quoted uncertainties, but the systematic uncertainties are approximately twice as large.

To measure the ratio ω, we also need to determine the two-particle BE correlation function $R_2(Q)$. This is done in the same way as the three-particle BE correlation function. The correlation function R_2 is parametrized as a Gaussian:

$$R_2(Q) = \gamma \left[1 + \lambda \exp(-R^2Q^2)\right] (1 + \varepsilon Q) \quad . \tag{14}$$

The parametrization starts at $Q = 0.08$ GeV, consistent with the study of R_3 from $Q_3 = 0.16$ GeV. The fit results[2)] are given in the first column of Table 3 and in Figure 2c.

If the space-time structure of the pion source is Gaussian and the pion production mechanism is completely incoherent, $\tilde{\lambda}$ and $\tilde{R}$ as derived from the fit to Equation (13) measure the same correlation strength and effective source size as λ and R of Equation (14). The values of λ and R are consistent with $\tilde{\lambda}$ and $\tilde{R}$, as expected for fully incoherent production of pions ($\omega = 1$). Using the values of λ and R instead of $\tilde{\lambda}$ and $\tilde{R}$ in Equation (13), which is justified if $\omega = 1$, results in the dashed line in Figure 3a. It is only slightly different from the result of the fit to Equation (13), indicating that ω is indeed near unity.

Another way to see how well R_3^{genuine} corresponds to a completely incoherent pion production interpretation and a Gaussian source density in space-time, is to compute ω with Equation (8), for each bin in Q_3 (from 0.16 to 0.80 GeV), using the measured R_3^{genuine} and R_2 derived from the parametrization of Equation (14). The result is shown in Figure 4a. At low Q_3, ω appears to be higher than unity.

Extended Gaussian Parametrizations

However, the assumption of a Gaussian source density is only an approximation, as observed in Reference 2 and confirmed by the χ^2 of the fit to Equation (14). Deviations from a Gaussian can be studied by expanding in terms of derivatives of the Gaussian, which are related to Hermite polynomials. Taking only the lowest-order non-Gaussian term into account, this so-called Edgeworth expansion [25] replaces the parametrization of Equation (14) by

$$R_2(Q) = \gamma \left[1 + \lambda \exp(-R^2Q^2)(1 + \kappa H_3(\sqrt{2}RQ)/6)\right] (1 + \varepsilon Q) \quad , \tag{15}$$

where κ measures the deviation from the Gaussian and $H_3(x) \equiv x^3 - 3x$ is the third-order Hermite polynomial. The fit results for the two-particle BE correlation function with this parametrization are given in the second column of Table 3.

Using the first-order Edgeworth expansion of the Gaussian, Equation (15), and using Equation (8), assuming $\omega = 1$, the parametrization of Equation (13) becomes

$$\begin{aligned} R_3^{\text{genuine}}(Q_3) &= \tilde{\gamma} \left(1 + 2\tilde{\lambda}^{1.5} \exp(-\tilde{R}^2Q_3^2/2) \left[\prod_{i,j=1,\, j>i}^{3} \sqrt{1 + \frac{H_3(\sqrt{2}\tilde{R}Q_{ij})}{6}\tilde{\kappa}}\,\right]\right) (1 + \tilde{\varepsilon}Q_3) \\ &\simeq \tilde{\gamma} \left(1 + 2\tilde{\lambda}^{1.5} \exp(-\tilde{R}^2Q_3^2/2) \left[1 + \frac{H_3(\sqrt{2}\tilde{R}Q_3/2)}{6}\tilde{\kappa}\right]^{1.5}\right) (1 + \tilde{\varepsilon}Q_3) \quad . \end{aligned} \tag{16}$$

In the second line the approximation is made that $Q_{ij} = Q_3/2$. The effect of this approximation on R_3^{genuine} is small compared to the statistical uncertainty. The results of a fit to Equation (16) are given in the second column of Table 1. The uncertainties are summarized in Table 2.

[2)] Due to the use of a different fit range, these fit results differ from those found in Reference 24. The same fit range gives similar results.

For both R_3^{genuine} and R_2, a better χ^2/NDF is found using the Edgeworth expansion, and the values of $\tilde{\lambda}$ and λ are significantly higher, as shown in Tables 1 and 3 and in Figures 3b and 2c. The values for $\tilde{\lambda}$ and $\tilde{R}$ are still consistent with the corresponding λ and R, as would be expected for a fully incoherent production mechanism of pions.

In Figure 3b, as in Figure 3a, we observe good agreement between the fit of R_3^{genuine} using the parametrization of Equation (16) and the prediction of a completely incoherent pion production mechanism, derived from parametrizing R_2 with Equation (15), over the full range of Q_3. In Figure 4b, no deviation from unity is observed for the ratio ω. This indicates that the data agree with the assumption of fully incoherent pion production.

Fits to samples generated with JETSET with BE effects modelled by BE_0 or BE_{32}[3)] [16] result in values of $\tilde{R}$ in agreement with the data but in significantly higher values of $\tilde{\lambda}$. This confirms the observation in Figure 1f that the standard BE implementations of JETSET overestimate the genuine three-particle BEC.

Summary

Three-particle, as well as two-particle Bose-Einstein correlations of like-sign charged pions have been measured in hadronic Z decay. Genuine three-particle BE correlations are observed. The correlation functions are better parametrized by an Edgeworth expansion of a Gaussian than by a simple Gaussian. Combining the two- and three-particle correlations shows that the data are consistent with a fully incoherent production mechanism of pions.

Acknowledgements

Clarifying discussions with T. Csörgő are gratefully acknowledged.

References

[1] DELPHI Collab., P. Abreu *et al.*, Phys. Lett. **B 286** (1992) 201; Z. Phys. **C 63** (1994) 17; ALEPH Collab., D. Decamp *et al.*, Z. Phys. **C 54** (1992) 75; OPAL Collab., G. Alexander *et al.*, Z. Phys. **C 72** (1996) 389.

[2] L3 Collab., M. Acciarri *et al.*, Phys. Lett. **B 458** (1999) 517.

[3] OPAL Collab., G. Abbiendi *et al.*, Eur. Phys. J. **C 16** (2000) 423; DELPHI Collab., P. Abreu *et al.*, Phys. Lett. **B 471** (2000) 460.

[4] G. Goldhaber *et al.*, Phys. Rev. **120** (1960) 300; D.H. Boal, C.K. Gelbke, B.K. Jennings, Rev. Mod. Phys. **62** (1990) 553.

[5] M. Biyajima *et al.*, Progr. Theor. Phys. **84** (1990) 931.

[6] H. Heiselberg and A.P. Vischer, Phys. Rev. **C 55** (1997) 874 and Preprint nucl-th/9707036 (1997).

[7] U. Heinz, and Q. Zhang, Phys. Rev. **C 56** (1997) 426.

[3)] The BE_{32} algorithm uses the values PARJ(92)=1.68 and PARJ(93)=0.38 GeV.

[8] B. Lörstad, Int. J. Mod. Phys. **A 4** (1989) 2861.

[9] I.V. Andreev, M. Plümer and R.M. Weiner, Int. J. Mod. Phys. **A 8** (1993) 4577.

[10] DELPHI Collab., P. Abreu *et al.*, Phys. Lett. **B 355** (1995) 415.

[11] OPAL Collab., K. Ackerstaff *et al.*, Eur. Phys. J. **C 5** (1998) 239.

[12] L3 Collab., B. Adeva *et al.*, Nucl. Instr. Meth. **A 289** (1990) 35; J.A. Bakken *et al.*, Nucl. Instr. Meth. **A 275** (1989) 81; O. Adriani *et al.*, Nucl. Instr. Meth. **A 302** (1991) 53; O. Adriani *et al.*, Phys. Reports **236** (1993) 1; B. Adeva *et al.*, Nucl. Instr. Meth. **A 323** (1992) 109; K. Deiters *et al.*, Nucl. Instr. Meth. **A 323** (1992) 162; M. Chemarin *et al.*, Nucl. Instr. Meth. **A 349** (1994) 345; M. Acciarri *et al.*, Nucl. Instr. Meth. **A 351** (1994) 300; I.C. Brock *et al.*, Nucl. Instr. Meth. **A 381** (1996) 23; A. Adam *et al.*, Nucl. Instr. Meth. **A 383** (1996) 342; G. Basti *et al.*, Nucl. Instr. Meth. **A 374** (1996) 293.

[13] T. Sjöstrand, Comp. Phys. Comm. **82** (1994) 74.

[14] G. Marchesini and B.R. Webber, Nucl. Phys. **B 310** (1988) 461; G. Marchesini *et al.*, Comp. Phys. Comm. **67** (1992) 465.

[15] L. Lönnblad and T. Sjöstrand, Phys. Lett. **B 351** (1995) 293.

[16] L. Lönnblad and T. Sjöstrand, Eur. Phys. J. **C 2** (1998) 165.

[17] R. Brun *et al.*, CERN report CERN DD/EE/84-1 (1984); revised 1987.

[18] H. Fesefeldt, RWTH Aachen report PITHA 85/02 (1985).

[19] V.L. Lyuboshitz, Sov. J. Nucl. Phys. **53** (1991) 514.

[20] T. Csörgő *et al.*, Eur. Phys. J. **C 9** (1999) 275.

[21] NA22 Collab., N.M. Agababyan *et al.*, Z. Phys. **C 68** (1995) 229.

[22] M. Gyulassy, S. Kauffmann, L.W. Wilson, Phys. Rev. **C 20** (1979) 2267.

[23] E.O. Alt *et al.*, Eur. Phys. J. **C 13** (2000) 663.

[24] L3 Collab., P. Achard *et al.*, Phys. Lett. **B 524** (2002) 55.

[25] F.Y. Edgeworth, Trans. Cambridge Phil. Soc. **20** (1905) 36. See also, e.g., Harald Cramér, Mathematical Methods of Statistics (Princeton Univ. Press, 1946); T. Csörgő and S. Hegyi, Phys. Lett. **B 489** (2000) 15.

The L3 Collaboration:

P.Achard,[21] O.Adriani,[18] M.Aguilar-Benitez,[25] J.Alcaraz,[25,19] G.Alemanni,[23] J.Allaby,[19] A.Aloisio,[29] M.G.Alviggi,[29] H.Anderhub,[47] V.P.Andreev,[6,34] F.Anselmo,[9] A.Arefiev,[28] T.Azemoon,[3] T.Aziz,[10,19] P.Bagnaia,[39] A.Bajo,[25] G.Baksay,[26] L.Baksay,[26] S.V.Baldew,[2] S.Banerjee,[10] Sw.Banerjee,[4] A.Barczyk,[47,45] R.Barillère,[19] P.Bartalini,[23] M.Basile,[9] N.Batalova,[44] R.Battiston,[33] A.Bay,[23] F.Becattini,[18] U.Becker,[14] F.Behner,[47] L.Bellucci,[18] R.Berbeco,[3] J.Berdugo,[25] P.Berges,[14] B.Bertucci,[33] B.L.Betev,[47] M.Biasini,[33] M.Biglietti,[29] A.Biland,[47] J.J.Blaising,[4] S.C.Blyth,[35] G.J.Bobbink,[2] A.Böhm,[1] L.Boldizsar,[13] B.Borgia,[39] S.Bottai,[18] D.Bourilkov,[47] M.Bourquin,[21] S.Braccini,[21] J.G.Branson,[41] F.Brochu,[4] J.D.Burger,[14] W.J.Burger,[33] X.D.Cai,[14] M.Capell,[14] G.Cara Romeo,[9] G.Carlino,[29] A.Cartacci,[18] J.Casaus,[25] F.Cavallari,[39] N.Cavallo,[36] C.Cecchi,[33] M.Cerrada,[25] M.Chamizo,[21] Y.H.Chang,[49] M.Chemarin,[24] A.Chen,[49] G.Chen,[7] G.M.Chen,[7] H.F.Chen,[22] H.S.Chen,[7] G.Chiefari,[29] L.Cifarelli,[40] F.Cindolo,[9] I.Clare,[14] R.Clare,[38] G.Coignet,[4] N.Colino,[25] S.Costantini,[39] B.de la Cruz,[25] S.Cucciarelli,[33] J.A.van Dalen,[31] R.de Asmundis,[29] P.Déglon,[21] J.Debreczeni,[13] A.Degré,[4] K.Dehmelt,[26] K.Deiters,[45] D.della Volpe,[29] E.Delmeire,[21] P.Denes,[37] F.DeNotaristefani,[39] A.De Salvo,[47] M.Diemoz,[39] M.Dierckxsens,[2] C.Dionisi,[39] M.Dittmar,[47,19] A.Doria,[29] M.T.Dova,[11,♯] D.Duchesneau,[4] B.Echenard,[21] A.Eline,[19] H.El Mamouni,[24] A.Engler,[35] F.J.Eppling,[14] A.Ewers,[1] P.Extermann,[21] M.A.Falagan,[25] S.Falciano,[39] A.Favara,[32] J.Fay,[24] O.Fedin,[34] M.Felcini,[47] T.Ferguson,[35] H.Fesefeldt,[1] E.Fiandrini,[33] J.H.Field,[21] F.Filthaut,[31] P.H.Fisher,[14] W.Fisher,[37] I.Fisk,[41] G.Forconi,[14] K.Freudenreich,[47] C.Furetta,[27] Yu.Galaktionov,[28,14] S.N.Ganguli,[10] P.Garcia-Abia,[5,19] M.Gataullin,[32] S.Gentile,[39] S.Giagu,[39] Z.F.Gong,[22] G.Grenier,[24] O.Grimm,[47] M.W.Gruenewald,[17] M.Guida,[40] R.van Gulik,[2] V.K.Gupta,[37] A.Gurtu,[10] L.J.Gutay,[44] D.Haas,[5] R.Sh.Hakobyan,[31] D.Hatzifotiadou,[9] T.Hebbeker,[1] A.Hervé,[19] J.Hirschfelder,[35] H.Hofer,[47] M.Hohlmann,[26] G.Holzner,[47] S.R.Hou,[49] Y.Hu,[31] B.N.Jin,[7] L.W.Jones,[3] P.de Jong,[2] I.Josa-Mutuberría,[25] D.Käfer,[1] M.Kaur,[15] M.N.Kienzle-Focacci,[21] J.K.Kim,[43] J.Kirkby,[19] W.Kittel,[31] A.Klimentov,[14,28] A.C.König,[31] M.Kopal,[44] V.Koutsenko,[14,28] M.Kräber,[47] R.W.Kraemer,[35] W.Krenz,[1] A.Krüger,[46] A.Kunin,[14] P.Ladron de Guevara,[25] I.Laktineh,[24] G.Landi,[18] M.Lebeau,[19] A.Lebedev,[14] P.Lebrun,[24] P.Lecomte,[47] P.Lecoq,[19] P.Le Coultre,[47] J.M.Le Goff,[19] R.Leiste,[46] M.Levtchenko,[27] P.Levtchenko,[34] C.Li,[22] S.Likhoded,[46] C.H.Lin,[49] W.T.Lin,[49] F.L.Linde,[2] L.Lista,[29] Z.A.Liu,[7] W.Lohmann,[46] E.Longo,[39] Y.S.Lu,[7] K.Lübelsmeyer,[1] C.Luci,[39] L.Luminari,[39] W.Lustermann,[47] W.G.Ma,[22] L.Malgeri,[21] A.Malinin,[28] C.Maña,[25] D.Mangeol,[31] J.Mans,[37] J.P.Martin,[24] F.Marzano,[39] K.Mazumdar,[10] R.R.McNeil,[6] S.Mele,[19,29] L.Merola,[29] M.Meschini,[18] W.J.Metzger,[31] A.Mihul,[12] H.Milcent,[19] G.Mirabelli,[39] J.Mnich,[1] G.B.Mohanty,[10] G.S.Muanza,[24] A.J.M.Muijs,[2] B.Musicar,[41] M.Musy,[39] S.Nagy,[16] S.Natale,[21] M.Napolitano,[29] F.Nessi-Tedaldi,[47] H.Newman,[32] T.Niessen,[1] A.Nisati,[39] H.Nowak,[46] R.Ofierzynski,[47] G.Organtini,[39] C.Palomares,[19] D.Pandoulas,[1] P.Paolucci,[29] R.Paramatti,[39] G.Passaleva,[18] S.Patricelli,[29] T.Paul,[11] M.Pauluzzi,[33] C.Paus,[14] F.Pauss,[47] M.Pedace,[39] S.Pensotti,[27] D.Perret-Gallix,[4] B.Petersen,[31] D.Piccolo,[29] F.Pierella,[9] M.Pioppi,[33] P.A.Piroué,[37] E.Pistolesi,[27] V.Plyaskin,[28] M.Pohl,[21] V.Pojidaev,[18] J.Pothier,[19] D.O.Prokofiev,[44] D.Prokofiev,[34] J.Quartieri,[40] G.Rahal-Callot,[47] M.A.Rahaman,[10] P.Raics,[16] N.Raja,[10] R.Ramelli,[47] P.G.Rancoita,[27] R.Ranieri,[18] A.Raspereza,[46] P.Razis,[30] D.Ren,[47] M.Rescigno,[39] S.Reucroft,[11] S.Riemann,[46] K.Riles,[3] B.P.Roe,[3] L.Romero,[25] A.Rosca,[8] S.Rosier-Lees,[4] S.Roth,[1] C.Rosenbleck,[1] B.Roux,[31] J.A.Rubio,[19] G.Ruggiero,[18] H.Rykaczewski,[47] A.Sakharov,[47] S.Saremi,[6] S.Sarkar,[39] J.Salicio,[19] E.Sanchez,[25] M.P.Sanders,[31] C.Schäfer,[19] V.Schegelsky,[34] S.Schmidt-Kaerst,[1] D.Schmitz,[1] H.Schopper,[48] D.J.Schotanus,[31] G.Schwering,[1] C.Sciacca,[29] L.Servoli,[33] S.Shevchenko,[32] N.Shivarov,[42] V.Shoutko,[14] E.Shumilov,[28] A.Shvorob,[32] T.Siedenburg,[1] D.Son,[43] C.Souga,[24] P.Spillantini,[18] M.Steuer,[14] D.P.Stickland,[37] B.Stoyanov,[42] A.Straessner,[19] K.Sudhakar,[10] G.Sultanov,[42] L.Z.Sun,[22] S.Sushkov,[8] H.Suter,[47] J.D.Swain,[11] Z.Szillasi,[26,¶] X.W.Tang,[7] P.Tarjan,[16] L.Tauscher,[5] L.Taylor,[11] B.Tellili,[24] D.Teyssier,[24] C.Timmermans,[31] Samuel C.C.Ting,[14] S.M.Ting,[14] S.C.Tonwar,[10,19] J.Tóth,[13] C.Tully,[37] K.L.Tung,[7] J.Ulbricht,[47] E.Valente,[39] R.T.Van de Walle,[31] R.Vasquez,[44] V.Veszpremi,[26] G.Vesztergombi,[13] I.Vetlitsky,[28] D.Vicinanza,[40] G.Viertel,[47] S.Villa,[38] M.Vivargent,[4] S.Vlachos,[5] I.Vodopianov,[34] H.Vogel,[35] H.Vogt,[46] I.Vorobiev,[35,28] A.A.Vorobyov,[34] M.Wadhwa,[5] W.Wallraff,[1] X.L.Wang,[22] Z.M.Wang,[22] M.Weber,[1] P.Wienemann,[1] H.Wilkens,[31] S.Wynhoff,[37] L.Xia,[32] Z.Z.Xu,[22] J.Yamamoto,[3] B.Z.Yang,[22] C.G.Yang,[7] H.J.Yang,[3] M.Yang,[7] S.C.Yeh,[50] An.Zalite,[34] Yu.Zalite,[34] Z.P.Zhang,[22] J.Zhao,[22] G.Y.Zhu,[7] R.Y.Zhu,[32] H.L.Zhuang,[7] A.Zichichi,[9,19,20] B.Zimmermann,[47] M.Zöller.[1]

1 I. Physikalisches Institut, RWTH, D-52056 Aachen, FRG[§]
III. Physikalisches Institut, RWTH, D-52056 Aachen, FRG[§]
2 National Institute for High Energy Physics, NIKHEF, and University of Amsterdam, NL-1009 DB Amsterdam, The Netherlands
3 University of Michigan, Ann Arbor, MI 48109, USA
4 Laboratoire d'Annecy-le-Vieux de Physique des Particules, LAPP,IN2P3-CNRS, BP 110, F-74941 Annecy-le-Vieux CEDEX, France
5 Institute of Physics, University of Basel, CH-4056 Basel, Switzerland
6 Louisiana State University, Baton Rouge, LA 70803, USA
7 Institute of High Energy Physics, IHEP, 100039 Beijing, China[△]
8 Humboldt University, D-10099 Berlin, FRG[§]
9 University of Bologna and INFN-Sezione di Bologna, I-40126 Bologna, Italy
10 Tata Institute of Fundamental Research, Mumbai (Bombay) 400 005, India
11 Northeastern University, Boston, MA 02115, USA
12 Institute of Atomic Physics and University of Bucharest, R-76900 Bucharest, Romania
13 Central Research Institute for Physics of the Hungarian Academy of Sciences, H-1525 Budapest 114, Hungary[‡]
14 Massachusetts Institute of Technology, Cambridge, MA 02139, USA
15 Panjab University, Chandigarh 160 014, India.
16 KLTE-ATOMKI, H-4010 Debrecen, Hungary[¶]
17 Department of Experimental Physics, University College Dublin, Belfield, Dublin 4, Ireland
18 INFN Sezione di Firenze and University of Florence, I-50125 Florence, Italy
19 European Laboratory for Particle Physics, CERN, CH-1211 Geneva 23, Switzerland
20 World Laboratory, FBLJA Project, CH-1211 Geneva 23, Switzerland
21 University of Geneva, CH-1211 Geneva 4, Switzerland
22 Chinese University of Science and Technology, USTC, Hefei, Anhui 230 029, China[△]
23 University of Lausanne, CH-1015 Lausanne, Switzerland
24 Institut de Physique Nucléaire de Lyon, IN2P3-CNRS,Université Claude Bernard, F-69622 Villeurbanne, France
25 Centro de Investigaciones Energéticas, Medioambientales y Tecnológicas, CIEMAT, E-28040 Madrid, Spain♭
26 Florida Institute of Technology, Melbourne, FL 32901, USA
27 INFN-Sezione di Milano, I-20133 Milan, Italy
28 Institute of Theoretical and Experimental Physics, ITEP, Moscow, Russia
29 INFN-Sezione di Napoli and University of Naples, I-80125 Naples, Italy
30 Department of Physics, University of Cyprus, Nicosia, Cyprus
31 University of Nijmegen and NIKHEF, NL-6525 ED Nijmegen, The Netherlands
32 California Institute of Technology, Pasadena, CA 91125, USA
33 INFN-Sezione di Perugia and Università Degli Studi di Perugia, I-06100 Perugia, Italy
34 Nuclear Physics Institute, St. Petersburg, Russia
35 Carnegie Mellon University, Pittsburgh, PA 15213, USA
36 INFN-Sezione di Napoli and University of Potenza, I-85100 Potenza, Italy
37 Princeton University, Princeton, NJ 08544, USA
38 University of Californa, Riverside, CA 92521, USA
39 INFN-Sezione di Roma and University of Rome, "La Sapienza", I-00185 Rome, Italy
40 University and INFN, Salerno, I-84100 Salerno, Italy
41 University of California, San Diego, CA 92093, USA
42 Bulgarian Academy of Sciences, Central Lab. of Mechatronics and Instrumentation, BU-1113 Sofia, Bulgaria
43 The Center for High Energy Physics, Kyungpook National University, 702-701 Taegu, Republic of Korea
44 Purdue University, West Lafayette, IN 47907, USA
45 Paul Scherrer Institut, PSI, CH-5232 Villigen, Switzerland
46 DESY, D-15738 Zeuthen, FRG
47 Eidgenössische Technische Hochschule, ETH Zürich, CH-8093 Zürich, Switzerland
48 University of Hamburg, D-22761 Hamburg, FRG
49 National Central University, Chung-Li, Taiwan, China
50 Department of Physics, National Tsing Hua University, Taiwan, China
§ Supported by the German Bundesministerium für Bildung, Wissenschaft, Forschung und Technologie
‡ Supported by the Hungarian OTKA fund under contract numbers T019181, F023259 and T037350.
¶ Also supported by the Hungarian OTKA fund under contract number T026178.
♭ Supported also by the Comisión Interministerial de Ciencia y Tecnología.
♯ Also supported by CONICET and Universidad Nacional de La Plata, CC 67, 1900 La Plata, Argentina.
△ Supported by the National Natural Science Foundation of China.

parameter	Eq. (13)	Eq. (16)
$\tilde{\gamma}$	$0.96 \pm 0.03 \pm 0.02$	$0.95 \pm 0.03 \pm 0.02$
$\tilde{\lambda}$	$0.47 \pm 0.07 \pm 0.03$	$0.75 \pm 0.10 \pm 0.03$
$\tilde{R}$, fm	$0.65 \pm 0.06 \pm 0.03$	$0.72 \pm 0.08 \pm 0.03$
$\tilde{\varepsilon}$, GeV^{-1}	$0.02 \pm 0.02 \pm 0.02$	$0.02 \pm 0.02 \pm 0.02$
$\tilde{\kappa}$	-	$0.79 \pm 0.26 \pm 0.15$
χ^2/NDF	29.9/27	17.7/26

Table 1: Values of the fit parameters for the genuine three-particle BE correlation function R_3^{genuine}, using the parametrizations of Equations (13) and (16). The first uncertainty corresponds to σ_1, the second to σ_2, defined in the text.

parametrization	Eq. (13)				Eq. (16)				
fit parameter	$\tilde{\gamma}$	$\tilde{\lambda}$	$\tilde{R}$, fm	$\tilde{\varepsilon}$, GeV^{-1}	$\tilde{\gamma}$	$\tilde{\lambda}$	$\tilde{R}$, fm	$\tilde{\varepsilon}$, GeV^{-1}	$\tilde{\kappa}$
σ_1 (stat.+modeling)	0.029	0.071	0.056	0.022	0.031	0.103	0.078	0.024	0.26
mixing	0.004	0.006	0.009	0.007	0.010	0.009	0.011	0.011	0.04
fit range	0.008	0.019	0.020	0.013	0.010	0.022	0.017	0.019	0.14
track/event sel.	0.010	0.013	0.012	0.008	0.011	0.016	0.012	0.007	0.10
$\delta\phi + \delta\theta$ cut	0.013	0.014	0.012	0.009	0.014	0.017	0.010	0.008	0.11
σ_2	0.019	0.028	0.028	0.020	0.023	0.033	0.026	0.024	0.15

Table 2: Contribution to the uncertainty on the fit parameters of the parametrizations of Equations (13) and (16), respectively. The first uncertainty corresponds to σ_1, the others added in quadrature give σ_2.

parameter	Eq. (14)	Eq. (15)
γ	$0.98 \pm 0.03 \pm 0.02$	$0.96 \pm 0.03 \pm 0.02$
λ	$0.45 \pm 0.06 \pm 0.03$	$0.72 \pm 0.08 \pm 0.03$
R, fm	$0.65 \pm 0.03 \pm 0.03$	$0.74 \pm 0.06 \pm 0.02$
ε, GeV^{-1}	$0.01 \pm 0.01 \pm 0.02$	$0.01 \pm 0.02 \pm 0.02$
κ	-	$0.74 \pm 0.21 \pm 0.15$
χ^2/NDF	60.2/29	26.0/28

Table 3: Values of the fit parameters for the two-particle BE correlation function, R_2, using the parametrizations of Equations (14) and (15). The first uncertainty corresponds to σ_1, the second to σ_2.

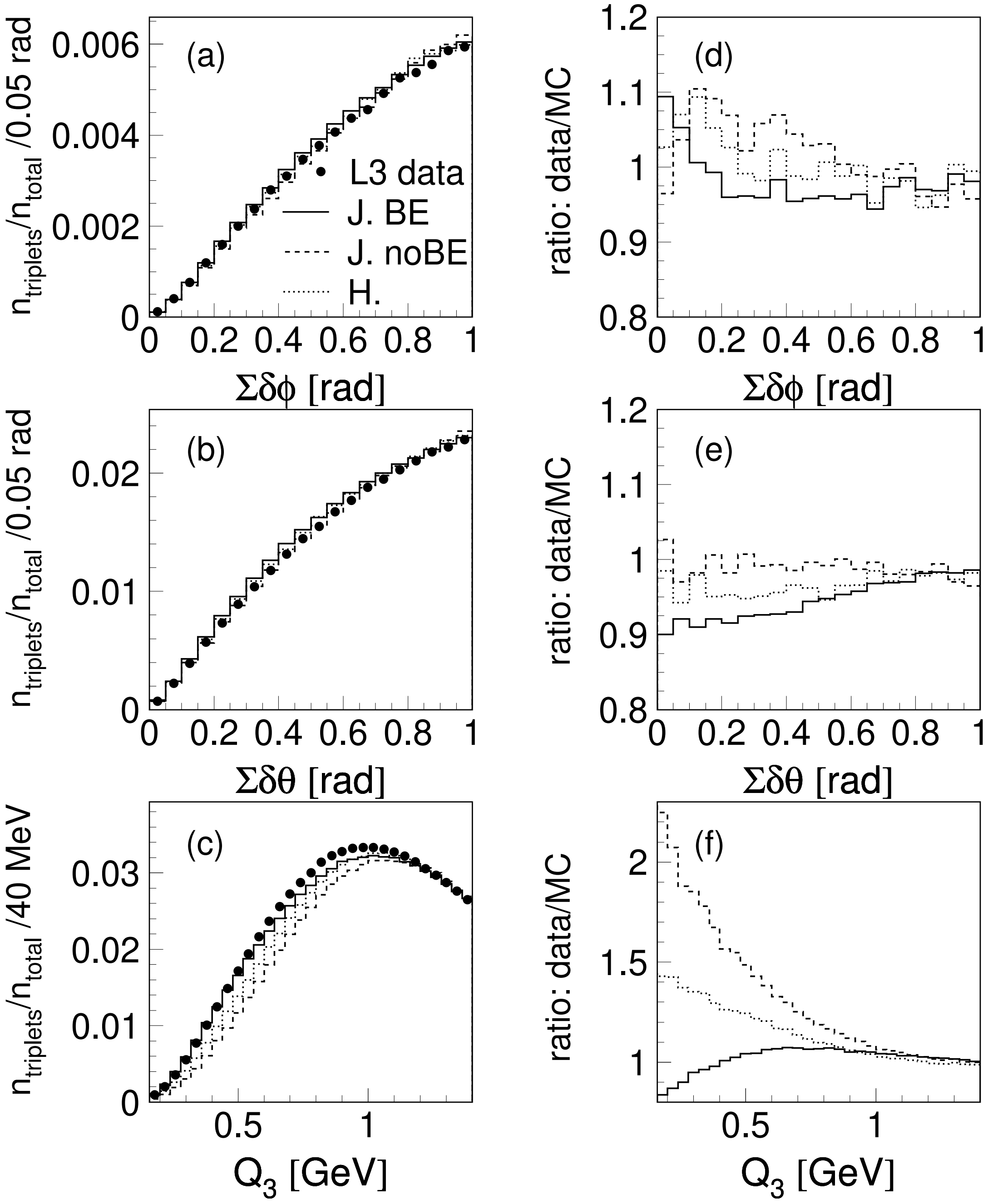

Figure 1: Normalized distributions of the sum of the difference in (a) azimuthal and (b) polar angle of pairs of tracks in a triplet, $\sum \delta\phi$ and $\sum \delta\theta$, and of (c) Q_3. Data, JETSET, with and without BE effects, and HERWIG are displayed. The ratios between the data and MC distributions are shown in (d), (e) and (f).

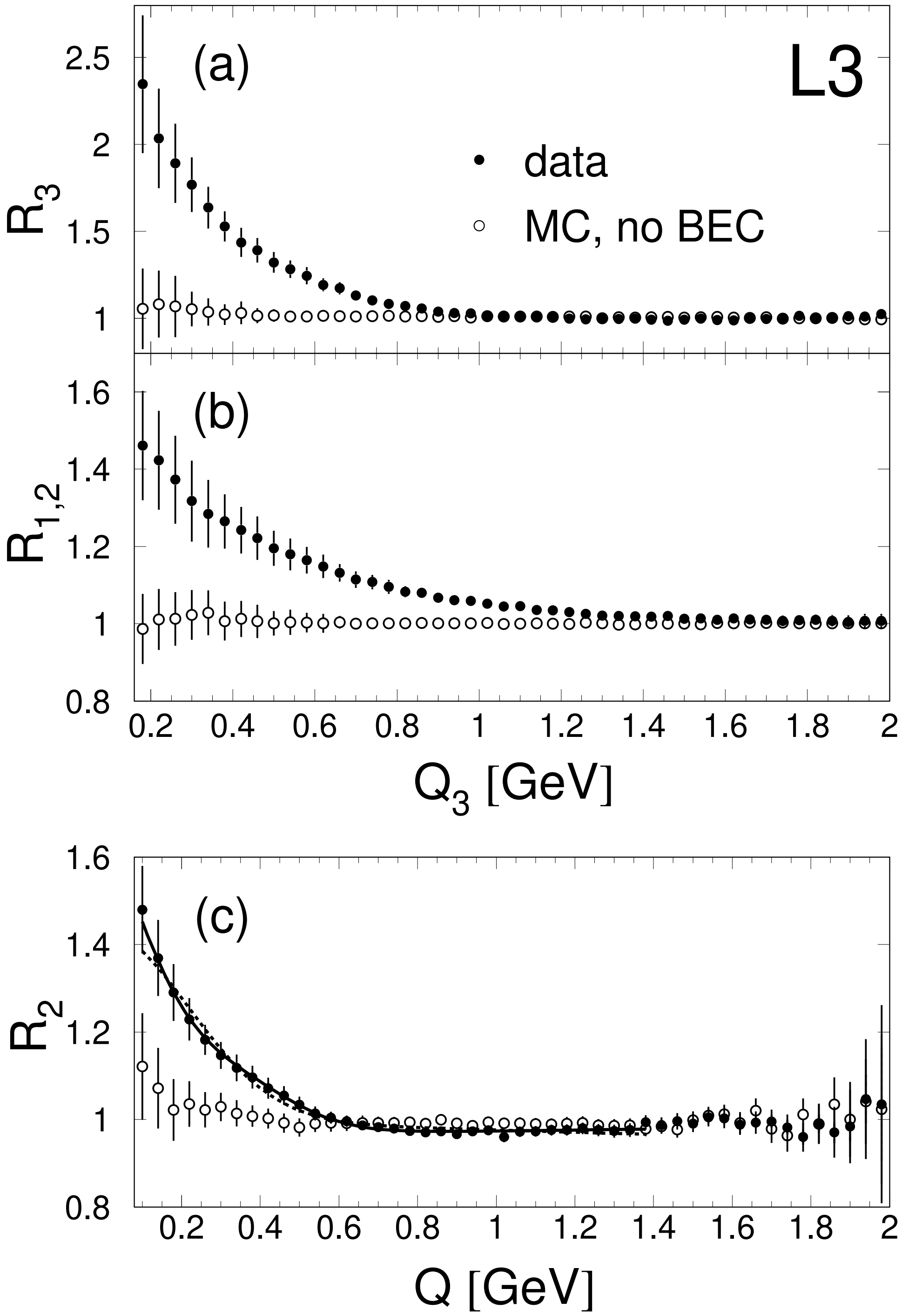

Figure 2: (a) The three-particle BE correlation function, R_3, from Equation (10), (b) the contribution of two-particle correlations, $R_{1,2} \equiv (\sum \rho_2\rho_1)/\rho_0 - 2$, and (c) R_2 from Equation (5). The full circles correspond to the data and the error bars to σ_1 (see text). The open circles correspond to the results from MC models without BEC. In (c) the dashed and full lines show the fits of Equations (14) and (15), respectively.

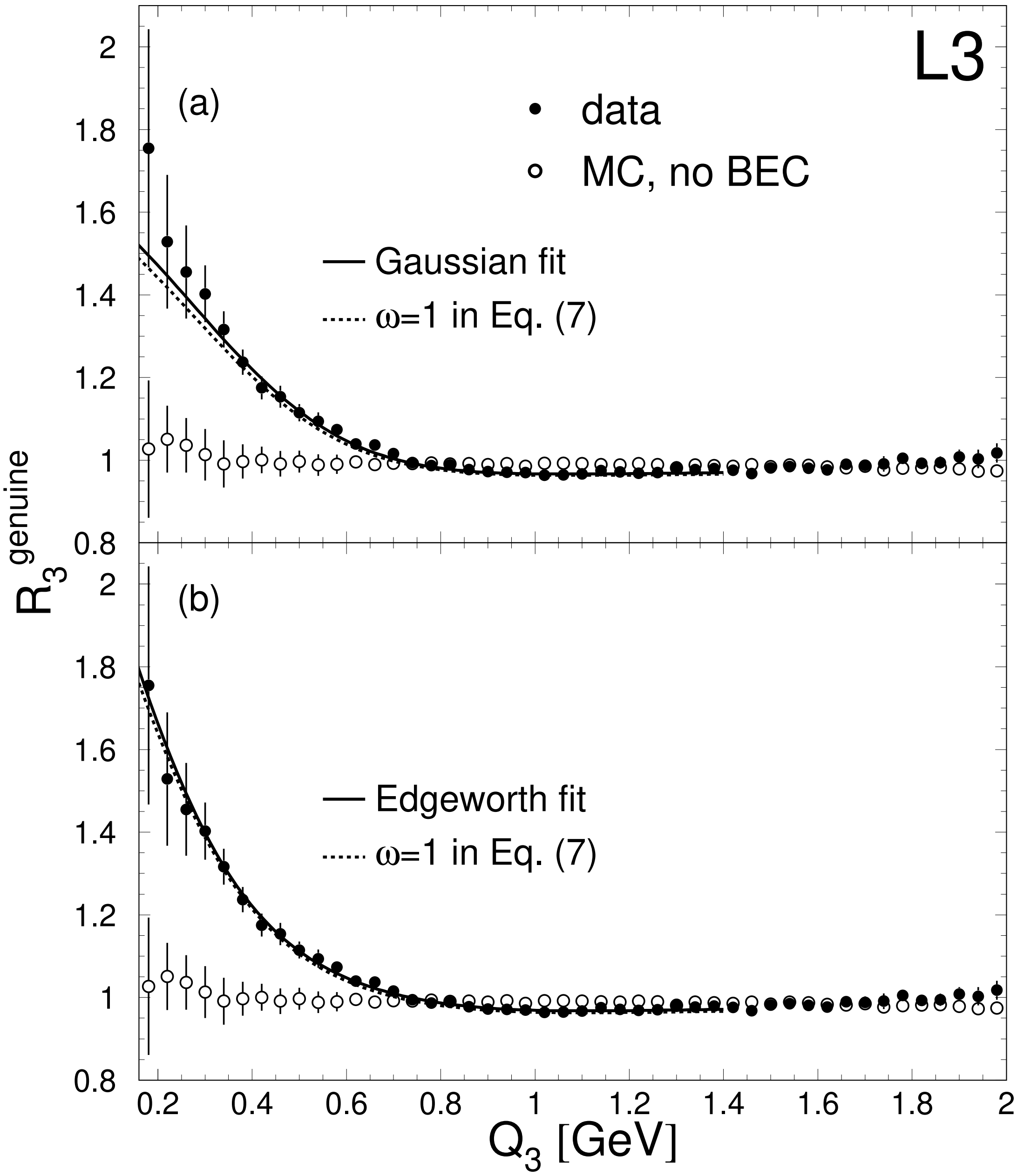

Figure 3: The genuine three-particle BE correlation function R_3^{genuine}, Equation (11). The full circles correspond to the data and the error bars to σ_1. The open circles correspond to results from MC models without BEC. In (a) the full line shows the fit of Equation (13), the dashed line the prediction of completely incoherent pion production and a Gaussian source density in space-time, derived from parametrizing R_2 with Equation (14). In (b) Equations (16) and (15) are used, respectively.

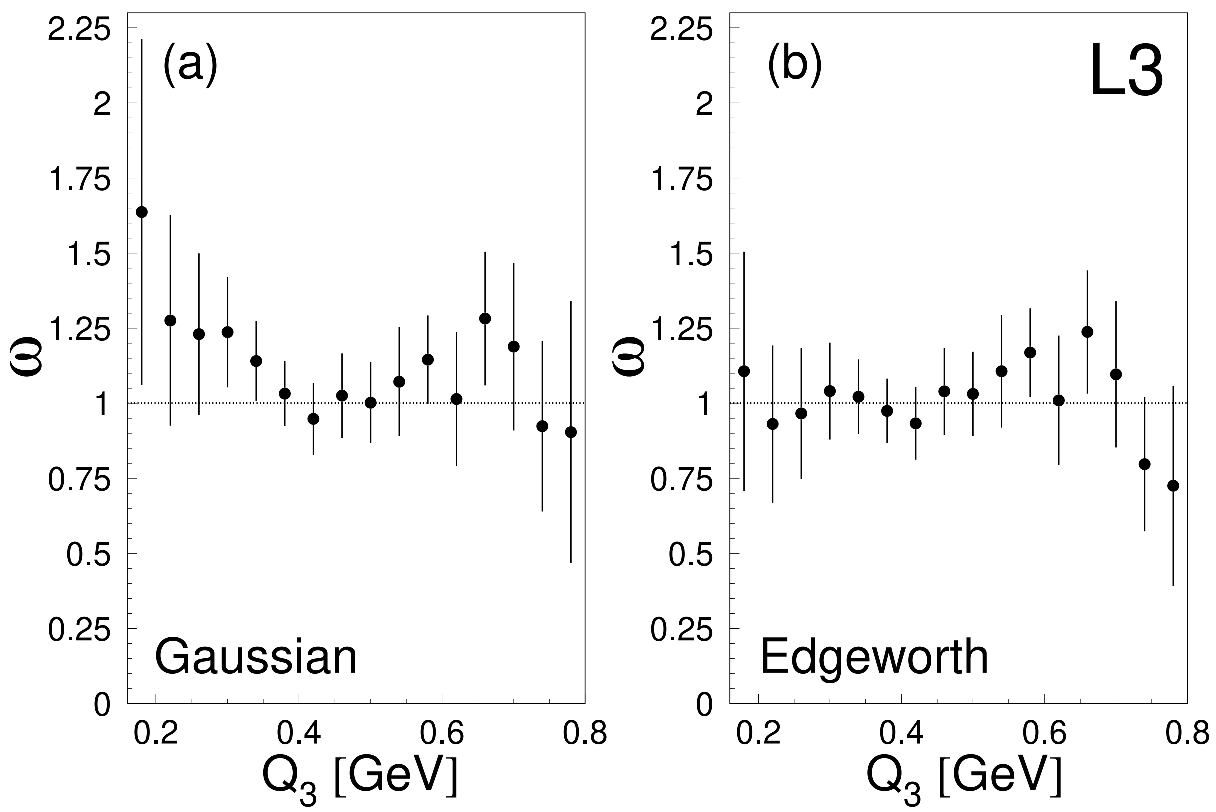

Figure 4: The ratio ω as a function of Q_3 assuming R_2 is described (a) by the Gaussian, Equation (14), and (b) by the first-order Edgeworth expansion of the Gaussian, Equation (15). The error bars correspond to σ_1. For completely incoherent production, $\omega = 1$.